

BIOLOGY CONTRIBUTION

ClonoScreen3D – A Novel 3-Dimensional Clonogenic Screening Platform for Identification of Radiosensitizers for Glioblastoma



Mark R. Jackson, DPhil,* Amanda R. Richards, MSc,* Abdul-Basit Ayoola Oladipupo, MSc,* Sandeep K. Chahal, MRes,* Seamus Caragher, MD, MPhil,*[†] Anthony J. Chalmers, MD, PhD,* and Natividad Gomez-Roman, PhD*[‡]

*Wolfson Wohl Cancer Research Centre, School of Cancer Sciences, University of Glasgow, Glasgow, UK; [†]Division of Plastic and Reconstructive Surgery, Department of Surgery, Massachusetts General Hospital, Massachusetts, USA; and [‡]Strathclyde Institute of Pharmacy and Biomedical Sciences, University of Strathclyde, Glasgow, UK

Received Oct 17, 2023; Accepted for publication Feb 18, 2024

Purpose: Glioblastoma (GBM) is a lethal brain tumor. Standard-of-care treatment comprising surgery, radiation, and chemotherapy results in median survival rates of 12 to 15 months. Molecular-targeted agents identified using conventional 2-dimensional (2D) in vitro models of GBM have failed to improve outcome in patients, rendering such models inadequate for therapeutic target identification. A previously developed 3D GBM in vitro model that recapitulates key GBM clinical features and responses to molecular therapies was investigated for utility for screening novel radiation-drug combinations using gold-standard clonogenic survival as readout.

Methods and Materials: Patient-derived GBM cell lines were optimized for inclusion in a 96-well plate 3D clonogenic screening platform, ClonoScreen3D. Radiation responses of GBM cells in this system were highly reproducible and comparable to those observed in low-throughput 3D assays. The screen methodology provided quantification of candidate drug single agent activity (half maximal effective concentration or EC₅₀) and the interaction between drug and radiation (radiation interaction ratio).

Results: The poly(ADP-ribose) polymerase inhibitors talazoparib, rucaparib, and olaparib each showed a significant interaction with radiation by ClonoScreen3D and were subsequently confirmed as true radiosensitizers by full clonogenic assay. Screening a panel of DNA damage response inhibitors revealed the expected propensity of these compounds to interact significantly with radiation (13/15 compounds). A second screen assessed a panel of compounds targeting pathways identified by transcriptomic analysis and demonstrated single agent activity and a previously unreported interaction with radiation of dinaciclib and cytarabine (radiation interaction ratio 1.28 and 1.90, respectively).

Corresponding author: Natividad Gomez-Roman, PhD; E-mail: natividad.gomez-roman@strath.ac.uk

Disclosures: none.

This work was funded by an NC3Rs grant (grant ref: [NC/P001335/1](https://doi.org/10.1016/j.ijrobp.2024.02.046)) awarded to N.G.-R. and A.J.C. Additional support was provided by the Cancer Research UK Radiation Research Centre of Excellence at the University of Glasgow ([C16583/A28803](https://doi.org/10.1016/j.ijrobp.2024.02.046)).

Data Sharing Statement: Research data are stored in an institutional repository and will be shared upon request to the corresponding author.

Acknowledgments—We would like to thank Prof. Colin Watts (University of Birmingham) and Dr Dimitris Placantonakis (NYU) who kindly donated cell lines. For the purpose of open access, the author(s) has applied a Creative Commons Attribution (CC BY) license to any author-accepted manuscript version arising from this submission.

Supplementary material associated with this article can be found in the online version at [doi:10.1016/j.ijrobp.2024.02.046](https://doi.org/10.1016/j.ijrobp.2024.02.046).

These compounds were validated as radiosensitizers in full clonogenic assays (sensitizer enhancement ratio 1.47 and 1.35, respectively).

Conclusions: The ClonoScreen3D platform was demonstrated to be a robust method to screen for single agent and radiation-drug combination activity. Using gold-standard clonogenicity, this assay is a tool for identification of radiosensitizers. We anticipate this technology will accelerate identification of novel radiation-drug combinations with genuine translational value. © 2024 The Author(s). Published by Elsevier Inc. This is an open access article under the CC BY license (<http://creativecommons.org/licenses/by/4.0/>)

Introduction

Glioblastoma (GBM) is the most common and most aggressive primary brain tumor.¹ Even with trimodal therapy comprising surgery, radiation, and chemotherapy (temozolomide),² prognosis remains dismal owing to marked chemo- and radioresistance.³ Multiple molecularly targeted agents exploiting pathways commonly dysregulated in GBM, including the receptor tyrosine kinase/Ras/phosphoinositide 3-kinase,³⁻⁵ α v integrins,⁶ p53, and retinoblastoma pathways, have shown therapeutic efficacy in preclinical models of GBM. However, all these agents have failed in the clinic, either alone or in combination with standard-of-care radiation therapy and/or chemotherapy.^{3,5,7,8} These results emphasize the need for improved experimental models that translate effectively to the clinic. A 3-dimensional (3D) in vitro GBM culture system that better reflects patient response to treatment was previously developed⁹ and extensively characterized in terms of cell morphology, mRNA and protein expression, and response to therapies, including radiation, chemotherapy (temozolomide), and clinically relevant molecular targeted agents (eg, erlotinib, bevacizumab). Comparison of the 3D system with conventional 2D or neurosphere models confirmed its superiority for drug discovery in GBM.¹⁰

Radiation therapy is a central component of GBM treatment and, although its efficacy in terms of overall survival has been proven in clinical trials,¹¹ tumor recurrence is seen in nearly all patients. Radiation dose escalation has not improved clinical outcomes, and most patients experience disabling neurocognitive toxicity. Enhancing the efficacy of radiation therapy will therefore require the use of radiosensitizing drugs that potentiate cytotoxicity in a tumor-specific manner.

Ionizing radiation (IR) generates DNA damage in the form of single-strand breaks and double-strand breaks (DSB). Detection of such damage leads to activation of the DNA damage response (DDR), which aims to preserve genomic integrity. DNA damage response signalling, for example that mediated by Ataxia-telangiectasia mutated (ATM), Ataxia Telangiectasia and Rad3-related protein (ATR) and Chk1, promotes cell cycle arrest and activation of DNA repair.¹² Single-strand breaks can be resolved through base excision repair and DSBs via homologous recombination (HR) or nonhomologous end-joining, among other pathways.^{13,14} Radioresistance in GBM has been linked to a subpopulation of cells termed “GBM stem-like cells,” which display preferential activation of the DDR and an increased DNA repair capacity.^{15,16} Pharmacologic disruption of the

DDR, when combined with radiation, therefore offers an attractive strategy to overcome radioresistance and enable radiation therapy to eliminate this clinically problematic population of tumor cells.

Identification of radiosensitizers in vitro is best achieved using the gold-standard clonogenic survival assay (CSA), but this is currently labor-intensive and time-consuming. Furthermore, limitations associated with compressing 2D CSAs to small growth area formats (eg, 96-well plate) because of colony size have presented a barrier.^{17,18} Nevertheless, in addition to nonclonogenic screening methods, efforts to establish clonogenic or pseudoclonegenic platforms have been made.¹⁷⁻²¹ However, development of a medium- or high-throughput clonogenic screen to identify radiosensitizers using primary GBM cells cultured in 3D conditions has not previously been reported.

To overcome these obstacles, we modified a clinically relevant 3D clonogenic system to 96-well plate format and observed that the high surface area of the 3D-Alvetex scaffold supported growth of sufficient numbers of colonies for large-scale compound screening. To identify novel, clinically exploitable targets for radiosensitization, we performed RNAseq analysis of GBM cells grown in 3D before and after radiation treatment. In addition to the expected DDR candidates, we identified novel potential targets in pathways including cell cycle progression, mitosis, and DNA synthesis. Our novel screening tool, the ClonoScreen3D platform, represents an improved experimental strategy for streamlining identification of novel radiosensitizers and has potential to transform the landscape of GBM therapy.

Methods and Materials

Cell culture and treatment

Patient-derived G7 and E2 GBM cells were obtained from Professor Colin Watts, as previously described.²² Gene mutations frequently observed in GBM in these cells are listed in [Table E1](#). Patient-derived GBML20 GBM cells were obtained from Dr Dimitris Placantonakis. Cells were cultured as monolayers on Matrigel-coated plates (0.2347 mg/mL in Adv/DMEM) in cancer stem cell enriching serum-free medium comprising Advanced/Dulbecco's Modified Eagle medium (DMEM)/F12 medium (GIBCO) supplemented with 1% B27 and 0.5% N2 (Thermo Fisher Scientific), 4 μ g/mL heparin, 10 ng/mL fibroblast growth factor 2 (Merck/Sigma),

20 ng/mL epidermal growth factor (Sigma) and 1% L-glutamine. G7s cells were grown in suspension conditions as spheres for routine passage and were then grown as monolayers on Matrigel-coated plates for 4 to 7 passages before seeding on 3D-Alvetex plates. G7m cells were maintained as monolayers on Matrigel-coated plates. Despite originating from the same parental line, these 2 models exhibit distinct features, including radiation responses. Cell lines were grown for a maximum of 7 passages before inclusion in experiments at 37 °C, with 5% CO₂. All cells were routinely monitored for mycoplasma contamination.

For 3D-Alvetex (Reprocell) cultures, plates were pre-treated according to the manufacturer's instructions (washed with 70% ethanol, followed by 3 washes with phosphate buffered saline (PBS)). 3D-Alvetex scaffolds were coated with Matrigel (0.2347 mg/mL), using 50 μL/well for 96-well 3D-Alvetex plates or 0.5 mL/well for 12-well 3D-Alvetex plates.

ClonoScreen3D clonogenic survival assay

Seeding densities were as follows: 180 cells/well for G7s and 150 cells/well for G7m cells. Eighteen hours after seeding, cells were treated with vehicle (dimethyl sulfoxide or DMSO) or inhibitor for 2 hours. Cells were irradiated (3 Gy) using an RS225 (XStrahl) x-ray cabinet, at 195 kV, 15 mA with a 0.5-mm copper filter, at a dose rate of 2.47 Gy/min, or sham-irradiated. Details of the inhibitor compounds are provided in Tables E2 and E3. Colonies were grown for 14 days at 37 °C, 5% CO₂, followed by incubation with thiazolyl blue tetrazolium bromide (MTT) for 4 hours at 37°C. Cells were fixed using 2% paraformaldehyde in PBS at room temperature for 15 min and washed with PBS.

Image acquisition and processing

High resolution images of plates were acquired using a photographic set-up comprising a white transilluminator to optimize contrast (Voliamart A3 Tracing Board) with a camera downward copy stand carrying a digital camera (Nikon D5300+ AF-P 18-55VR). Image capture was performed using digiCamControl software. Well segmentation was performed with ImageJ software. Colonies composed of >50 cells were counted either manually or in a semiautomated manner using the open-source software OpenCFU (<http://openfcu.sourceforge.net>).

Quantification of single agent activity and radiosensitizing potential

Colony counts were converted into surviving fraction (SF) using the plating efficiency of vehicle-treated cells for each radiation dose, thus correcting the values for the effect of IR.²³⁻²⁵ For determination of single agent activity, the mean

SFs of sham-irradiated replicates were calculated and modeled using a 4-parameter dose response curve using the drc package²⁵ in R (3.6.3; <https://www.R-project.org>). Single agent activity was expressed in terms of half maximal effective concentration (EC₅₀). For compounds that lacked single agent activity or did not conform to a classical dose response, EC₅₀ was not determined.

Radiosensitizing potential was quantified by calculation of a novel parameter: the radiation interaction ratio (RIR). The linear interpolation area under the curve (AUC) of SF against log₁₀(drug concentration) was computed for individual biologic replicates at each radiation dose using the MESS package.²³ The replicate AUCs were subjected to a ratio *t* test from the mratios package²⁴ with ratio under the null hypothesis $\rho = 1$, to determine the statistical significance of the interaction with IR. *P* values were adjusted for multiple comparison using the false discovery rate method. Thus, RIR was defined as

$$\frac{\frac{1}{n} \sum_i A_i^C}{\frac{1}{n} \sum_i A_i^R}; i = 1, \dots, n$$

where A^C is the AUC of the sham-irradiated control and A^R is the AUC of the irradiated sample. An example R script for computation of RIR can be found in the Supplementary Materials accompanying file. Where data conformed to a dose-response curve, the EC₅₀ values of the sham and irradiated samples were additionally compared by *t* test of coefficient ratio.

3D CSA for full radiation dose response

Twelve-well plate 3D-Alvetex CSAs were performed as previously described.²² Briefly, seeding densities for all cell line cells varied according to radiation dose: 300 cells/well for 0, 1, and 2 Gy; 500 cells/well for 3 Gy; 800 cells/well for 4 Gy; and 1000 cells/well for 5 Gy. Eighteen hours after seeding, cells were treated with vehicle (DMSO) or inhibitor for 2 hours at 37 °C (5% CO₂) and subsequently sham-irradiated or exposed to different radiation doses (1-5 Gy). Colonies were grown for 18 to 21 days at 37 °C, 5% CO₂, followed by incubation with MTT for 4 hours at 37°C and fixed with 2% paraformaldehyde in PBS at room temperature for 15 min and washed with PBS. Plates were stored in PBS at 4 °C, which was removed immediately before imaging and automated colony counting. Drug sensitizer enhancement ratios (SER) were calculated using mean inactivation doses determined from linear quadratic fits as described in Ekstrøm et al.²³

Gene expression analysis

Four days after plating cells in 3D conditions (3D-Alvetex), RNA was extracted with TRIzol reagent. RNAseq analysis was performed using the IlluminaNextSeq500 for a PolyA selection RNA library, with a paired-end sequencing model and 33M depth for triplicate experimental repeats of 2D

and 3D culture of G7m and E2 cells. RNAseq analysis was performed as previously described.⁹

Results

Optimization of the ClonoScreen3D platform

Five patient-derived GBM cell lines O6-methylguanine-DNA methyltransferase (MGMT) promoter methylated G7s, G7m, and E2, and MGMT promoter unmethylated S2 and GBML20 were used to evaluate the feasibility of converting the 3D CSA from 12-well format to 96-well format. G7s, G7m, and GBML20 cell lines formed distinct colonies with plating efficiencies of 30% to 50% compared with diffuse growth and low-plating efficiency (<20%) observed for E2 and S2 (Fig. 1A). Accordingly, further assay development was performed using G7s cells. Seeding density and colony growth times were optimized to obtain sufficient countable colonies under control and irradiated conditions. To validate the screen with radiation, G7s cells were exposed to 3 Gy (Fig. 1B), a dose selected based on survival responses to radiation alone and in combination with various compounds (rucaparib example shown in Fig. 1C). Colony forming ability and radiation/drug responses were not significantly affected by the transition to 96-well format.

To maximize efficiency, an automated colony counting process was developed using the open-source software packages ImageJ (<https://imagej.net/software/fiji/>) and OpenCFU²⁶ and compared against manual counting. Manual and automated counts showed a strong positive correlation, although some small differences in absolute values were noted (Spearman's rho 0.91; $P < .001$; Fig. E1). Importantly, using drug response as the critical endpoint, near identical responses to erlotinib (Fig. 1D) and AZD1775 (Fig. 1E) were observed, with or without radiation. These plots show data normalized for IR effects to highlight interactions between drug and radiation as shifts in drug response. Because only a single radiation dose was tested, we describe these plots as indicating radiosensitizing potential rather than radiosensitization per se, which generally requires multiple radiation dose points. Notably, the 96-well 3D-CSA enabled quantification of single agent activity (SAA) as well as IR interactions, thereby also informing selection of drug concentration(s) for further radiosensitization studies.

RIR to quantify interaction between drugs and radiation

Initial characterization of ClonoScreen3D used NU7441, a known radiosensitizer that inhibits the key DSB repair protein DNA-dependent protein kinase (DNA-PK).²⁷ Although NU7441 showed weak SAA in the G7s cell line (Fig. 1F), it exhibited the expected marked interaction with IR, as indicated by the shift in drug dose response curve.

Although SAA can be readily parameterized in terms of drug EC_{50} , no analysis method has been developed to quantify the interaction with radiation. For drugs exhibiting SAA, comparison of EC_{50} values for drug alone and in combination with IR is indicative of radiosensitizing activity.²⁸ However, this approach is not applicable when drugs lack SAA or do not conform to a classical dose response, as in Figure 1F (0 Gy), where EC_{50} cannot be estimated with meaningful confidence. In such situations, statistical comparison of EC_{50} values fails to capture even marked shifts in dose response (Fig. 1F; $P = 0.129$). To address this issue, we determined AUC values for control and irradiated samples, an approach inspired by the widely used mean inactivation dose parameter.²⁹ This generated a novel value, which we termed the “radiation interaction ratio” (RIR), which is defined as the ratio of AUCs and captures the relative shift in dose response curves, thus providing a quantitative readout of radiosensitizing potential. In the example shown in Figure 1F, the RIR was found to be 3.99 ($P = .016$), confirming statistical significance and quantifying the observed interaction between NU7441 and IR.

Quantification of radiosensitizing activity of poly (ADP-ribose) polymerase inhibitors using the ClonoScreen3D platform

Because the DNA repair enzyme poly(ADP-ribose) polymerase 1 (PARP-1) is overexpressed in GBM and shows very low expression in healthy brain tissue, it is a promising therapeutic target.³⁰ PARP inhibitors (PARPi) have consistently shown radiosensitizing effects in preclinical models of GBM both in vitro and in vivo³¹⁻³³ and are currently under investigation in phase I and II clinical trials.³⁴

To validate ClonoScreen3D as a radiosensitizer screening tool, we evaluated the radiation interactions of 3 PARPi: rucaparib, talazoparib, and olaparib, the latter 2 known to radiosensitize GBM.^{16,35} Using ClonoScreen3D, these compounds all exhibited radiation interactions in G7s cells (Fig. 2A), with talazoparib having the highest RIR value (RIR 2.53; $P < .001$), followed by rucaparib (RIR 1.95; $P = .002$) and olaparib (RIR 1.56; $P = .003$). Analysis by ClonoScreen3D also revealed that talazoparib exhibited potent SAA (EC_{50} 32 nmol/L; 95% CI, 27-37 nmol/L), unlike the other PARPi tested to date.

To confirm true radiosensitizing activity, PARPi were tested in 12-well 3D-CSA with multiple radiation dose (0-5 Gy). Based on ClonoScreen3D data, olaparib and rucaparib were dosed at 1 μ mol/L and talazoparib at 5 nmol/L owing to its potent SAA. As expected, all 3 PARPi caused significant radiosensitization (SER >1), confirming the ability of RIR to detect radiosensitizers (Fig. 2B, Table E4). Furthermore, RIR values exhibited a monotonic relationship with gold-standard SER in G7s cells across the 3 PARPi tested (Fig. 2C).

To assess the generalizability of RIR to identify GBM radiosensitizers, we determined RIR values for PARPi in a second GBM model (G7m), which had been optimized for

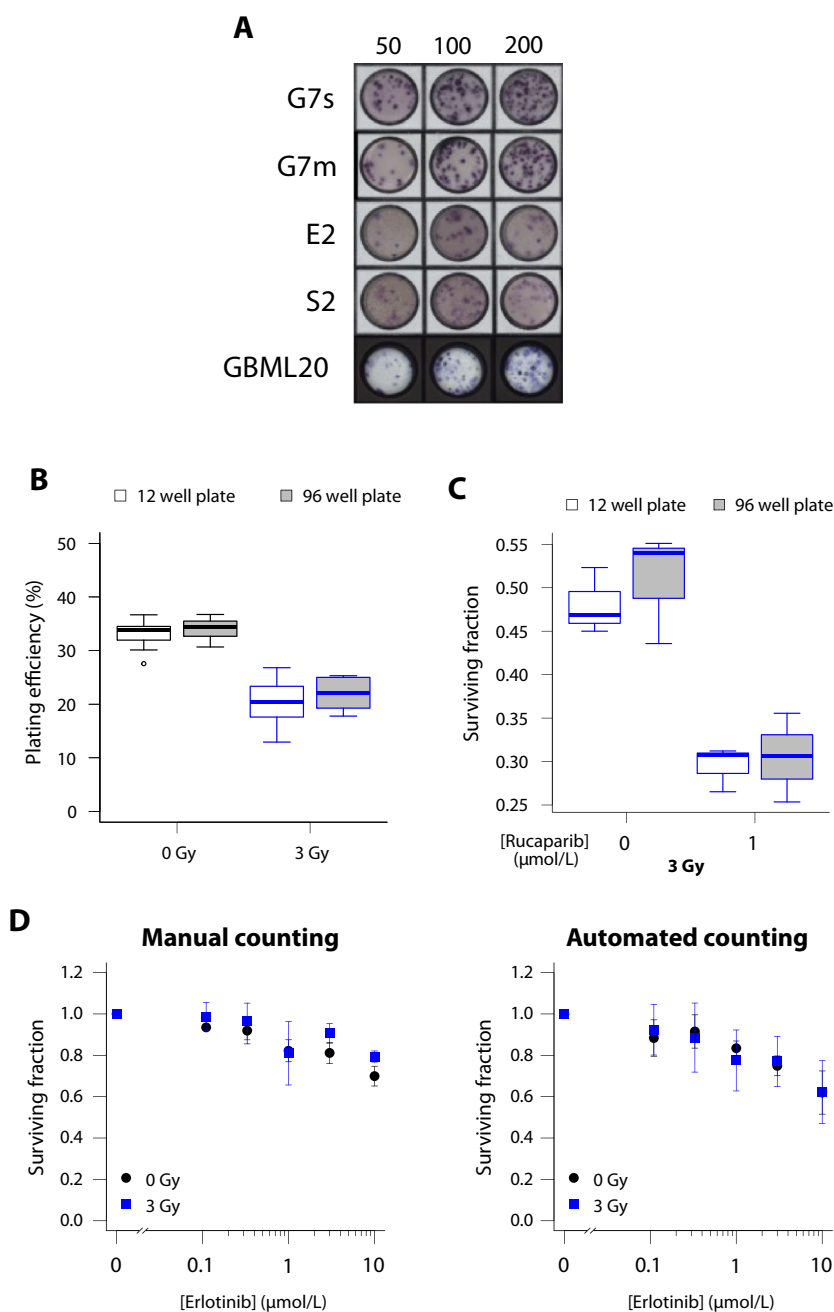


Fig. 1. Optimization of the ClonoScreen3D screening clonogenic assay format. (A) Representative images of thiazolyl blue tetrazolium bromide–stained and formalin fixed colonies of patient-derived cell lines G7s, G7m, E2, S2, and GBML20 seeded in 96-well 3D-Alvetex plates under stem-enriched conditions at 50, 100, and 200 cells per well, incubated for 14 days. (B) Clonogenic plating efficiency of G7s cells after sham irradiation or exposure to 3 Gy in 12- and 96-well clonogenic assay format, $n \geq 6$. (C) Clonogenic survival of G7s cells treated with 3 Gy alone or in combination with rucaparib (1 $\mu\text{mol/L}$) in 12- and 96-well clonogenic assay format, $n = 6$. Boxplots presented according to the Tukey method. (D) Clonogenic survival of G7s cells after treatment with erlotinib or vehicle 2 hours before ionizing radiation (3 Gy) calculated using manual or automated colony counting. (E) Clonogenic survival of G7s cells after treatment with AZD1775 or vehicle 2 hours before ionizing radiation (3 Gy) calculated using manual or automated colony counting. (F) Clonogenic survival of G7s cells after treatment with NU7441 or vehicle 2 hours before ionizing radiation (3 Gy) calculated from automated colony counts. The radiation interaction ratio is calculated by comparison of areas under the curve of the control (0 Gy) and irradiated (3 Gy) samples after log-transformation of concentration. The surviving fraction of irradiated samples was computed using the plating efficiency of the vehicle + 3 Gy control, normalizing for the effect of radiation alone. Points represent mean \pm SD, $n = 3$. Half maximal effective concentration or EC_{50} ($\mu\text{mol/L}$) with 95% CI calculated by fitting of a 4-parameter dose response curve. EC_{50} values compared by testing means of ratios.

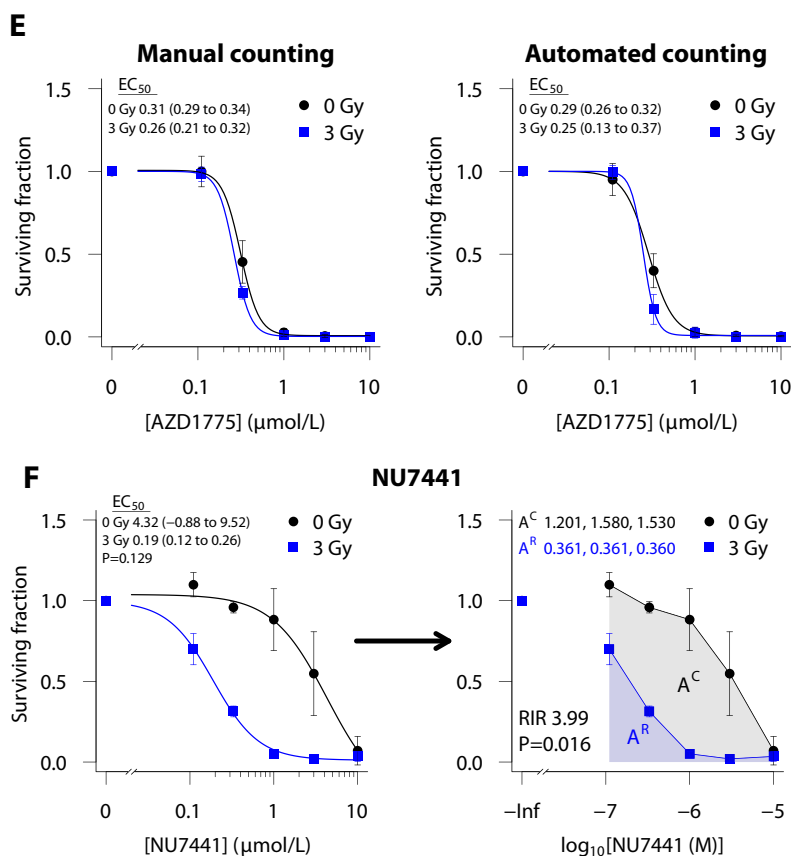


Fig. 1. Continued.

ClonoScreen3D (Fig. E2). Consistent with the previous result, talazoparib was the only PARPi to exhibit potent SAA (EC_{50} 76 nmol/L; 95% CI, 42-110 nmol/L) and also showed the greatest interaction with IR (RIR 1.96; $P = .003$), followed by rucaparib (RIR 1.37; $P = .004$) and olaparib (RIR 1.26; $P = .048$; Fig. 2D). Significant radiosensitization was observed in full CSA for each PARPi in G7m cells (Fig. 2E), which again correlated monotonically with RIR (Fig. 2F). Together, these findings demonstrate the utility of RIR for identification and prioritization of candidate radiosensitizers.

Quantitative comparison of radiosensitizing effects of different DDR inhibitors

Although the radiosensitizing activities of multiple DDR inhibitors have been studied individually, direct comparison of inhibitors targeting different pathways has not been widely reported. We screened 15 inhibitors targeting proteins involved in DDR processes including DNA repair and signaling (Table E2) using G7s cells and the ClonoScreen3D assay workflow summarized in Figure 3. Five compounds exhibited potent SAA ($EC_{50} < 2 \mu\text{mol/L}$; Fig. 4A,B; Table E5), with talazoparib displaying the highest activity, followed by inhibitors targeting Chk1/2 and ATR. Compounds were ranked by

RIR adjusted P value (Fig. 4A), to encapsulate both the magnitude and reproducibility of the interaction with IR. In addition to summary graphics, individual drug response curves are presented in Figures E3 and E4, and numerical results are reported in Tables E5 and E6.

To assess the specificity of the assay, an inactive control compound was included. PDD00031704 is a modified variant of a Poly (ADP-ribose) glycohydrolase (PARG) inhibitor, with on-target $EC_{50} > 100 \mu\text{mol/L}$. In the ClonoScreen3D assay, this compound ranked lowest for interaction with radiation in G7s and G7m cells (Figs. 4A,C and E4). In G7s cells, the ATM inhibitor AZD1390 exhibited a marked interaction with IR (RIR 2.98; $P < .001$), and the less potent ATM inhibitor KU55933 showed limited (nonsignificant) activity only at $10 \mu\text{mol/L}$ (Fig. 4D). The next highest ranked compound was SCH 900776, an inhibitor of Chk1/2 (RIR 1.85; $P = .013$; Fig. 4E), and another Chk1/2 inhibitor AZD7762 was also identified as a hit (RIR 2.47; $P = .017$). Two ATR inhibitors, AZD6738 (RIR 2.16; $P = .017$) and VX970 (RIR 2.33; $P = .017$), were also identified as interacting significantly with IR (Fig. 4F). The DNA-PK inhibitor NU7441 exhibited the greatest absolute interaction with IR (RIR 3.99; $P = .016$; Fig. 1F), although its ranking was reduced by inter-replicate variability. By contrast, a second DNA-PK inhibitor, NU7026, showed no significant activity. Two HR-targeting inhibitors exhibited

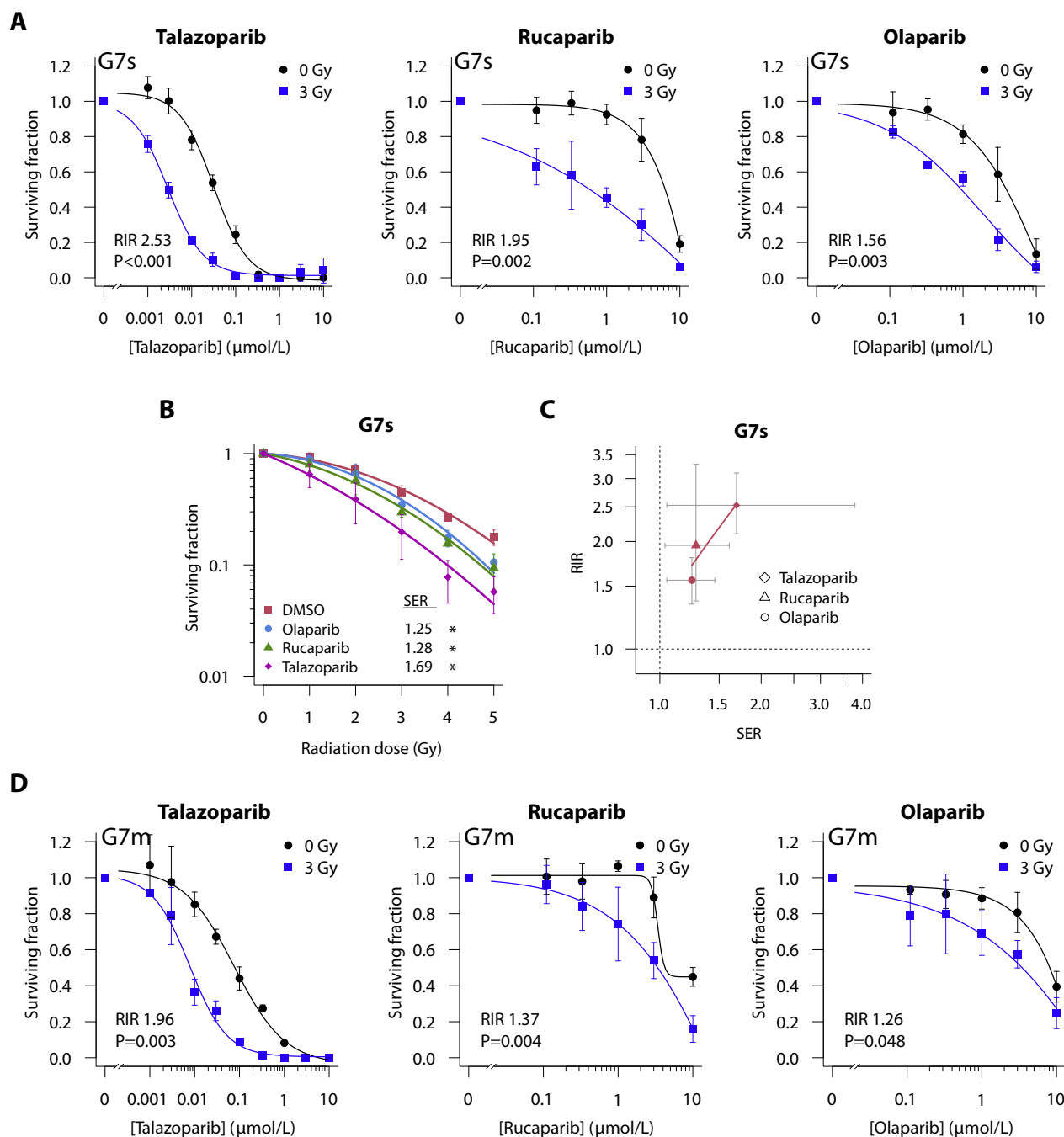


Fig. 2. Validation of the ClonoScreen3D platform for identification of radiosensitizers using PARP inhibitors. (A) Clonogenic survival of G7s cells after treatment with PARP inhibitors or vehicle 2 hours before IR (3 Gy). The surviving fraction of irradiated samples was computed using the plating efficiency of the vehicle + 3 Gy control, normalizing for the effect of radiation alone. Data fitted with a 4-parameter dose response curve. (B) Full 3-dimensional radiation dose response clonogenic survival of G7s cells treated with olaparib (1 $\mu\text{mol/L}$), rucaparib (1 $\mu\text{mol/L}$), and talazoparib (5 nmol/L) 2 hours before IR. Data fitted using the linear quadratic model. SER calculated using linear quadratic mean inactivation dose and subject to 1-tailed ratio *t* test. (C) Correlation of radiation interaction ratio and SER values determined for PARP inhibitors in G7s cells. Points represent values calculated from 3 independent experiments, and error bars indicate coefficient 95% CIs. (D) Clonogenic survival of G7m cells after treatment with PARP inhibitors or vehicle 2 hours before IR (3 Gy). The surviving fraction of irradiated samples was computed using the plating efficiency of the vehicle + 3 Gy control, normalizing for the effect of radiation alone. Data fitted with a 4-parameter dose response curve. (E) Full 3-dimensional radiation dose response clonogenic survival of G7m cells treated with olaparib (1 $\mu\text{mol/L}$), rucaparib (1 $\mu\text{mol/L}$), and talazoparib (5 nmol/L) 2 hours before IR. Data fitted using the linear quadratic model. SER calculated using linear quadratic mean inactivation dose and subject to 1-tailed ratio *t* test. (F) Correlation of radiation interaction ratio and SER values determined for PARP inhibitors in G7m cells. Points represent values calculated from 3 independent experiments, and error bars indicate coefficient 95% CIs. Unless otherwise stated, points represent mean \pm SD, *n* = 3. *Abbreviations:* IR = ionizing radiation; PARP = poly(ADP-ribose) polymerase; RIR = radiation interaction ratio; SER = sensitizer enhancement ratios.

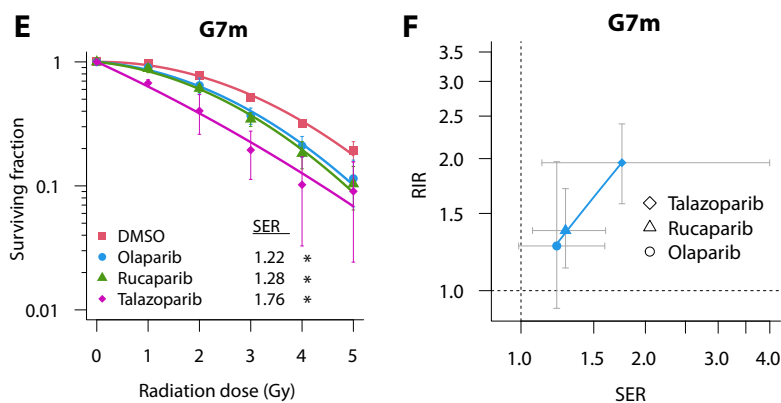


Fig. 2. Continued.

limited radiation interaction, which was statistically significant only for B02 (RIR 1.23; $P = .017$; Fig. 4G); this may be explained by their low drug potencies, having EC_{50} values in the micromolar range.

Of the 15 DDR inhibitors tested, 8 compounds showed a significant interaction with radiation in both G7s and G7m cells (Figs. 4A,D-G and E4). A further 5 compounds showed radiosensitizing potential in a single cell line.

Identification of novel targets for radiosensitization of GBM cells

To identify novel radiosensitization targets, we performed RNAseq analysis on samples obtained from 2 patient-derived GBM cell lines, E2 and G7m, that had been cultured

in 3D and treated with IR (5 Gy) or sham-irradiated 4 hours previously. The timepoint of RNA extraction was chosen to identify early response genes regulating radioresistance in GBM. Because only modest changes in gene expression were observed in E2 cells, we focused on G7m cells. In this context, exposure to IR significantly altered expression of multiple DDR genes (eg, BRCA1, RAD51, XRCC2) as expected, and also included genes associated with: (1) reduced cell cycle (CDC25C, CDKN1B, CDK18) and mitotic progression (BUB1, PLK1, CDC25A); (2) NF κ B signalling (NFKBIE, NFKBIA, and NFKB2); (3) cytokine and growth factor signalling (CXCL10, CXCL6, VEGFA); and (4) stem cell regulation (FOS, WNT2, WNT5A, ID4) (Fig. 5A). A full list is provided in File E1.

Commercially available inhibitors targeting pathways and gene products identified in this experiment were

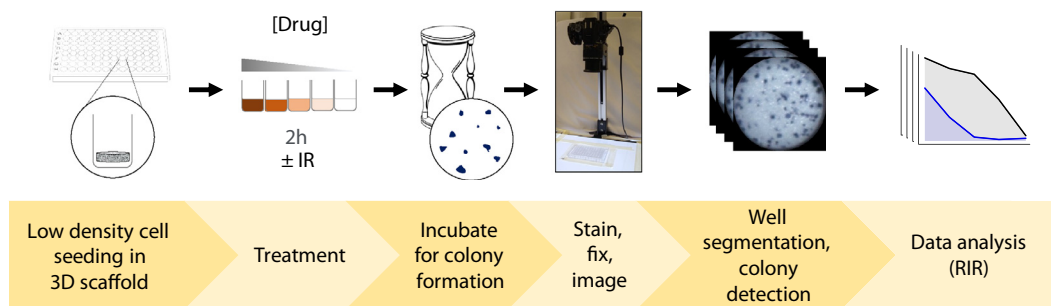


Fig. 3. Schematic depicting the workflow for ClonoScreen3D when screening compounds for interaction with radiation. Graphical description of the methodology for the ClonoScreen3D platform. ClonoScreen3D uses 96-well plates containing Alvetex 3-dimensional scaffolds made of highly porous polystyrene 200 microns in depth, in a stem cell-enriching environment allowing maintenance of chemo- and radioresistant cell populations by culturing cells in the absence of fetal calf serum and the presence of growth factors (epidermal growth factor and fibroblast growth factor) and supplements N2 and B27 (see Methods and Materials for concentrations). To support cell adherence, scaffolds are coated with diluted Matrigel (0.2347 mg/mL in Advanced/Dulbecco’s Modified Eagle Medium), as described in Methods and Materials. Cells are seeded onto scaffolds, incubated for 18 hours, and treated with respective compounds over the desired concentration range. After 2 hours incubation, cells are irradiated or sham-irradiated and incubated for colony formation. Colonies are stained with thiazolyl blue tetrazolium bromide and images of plates acquired with a digital camera followed by well segmentation using ImageJ and automated colony counting with OpenCFU. After normalization for the effect of ionizing radiation, radiation interaction ratios are determined. Compound single agent activity is additionally quantified in terms of half maximal effective concentration (EC_{50}), after fitting of a 4-parameter dose response model.

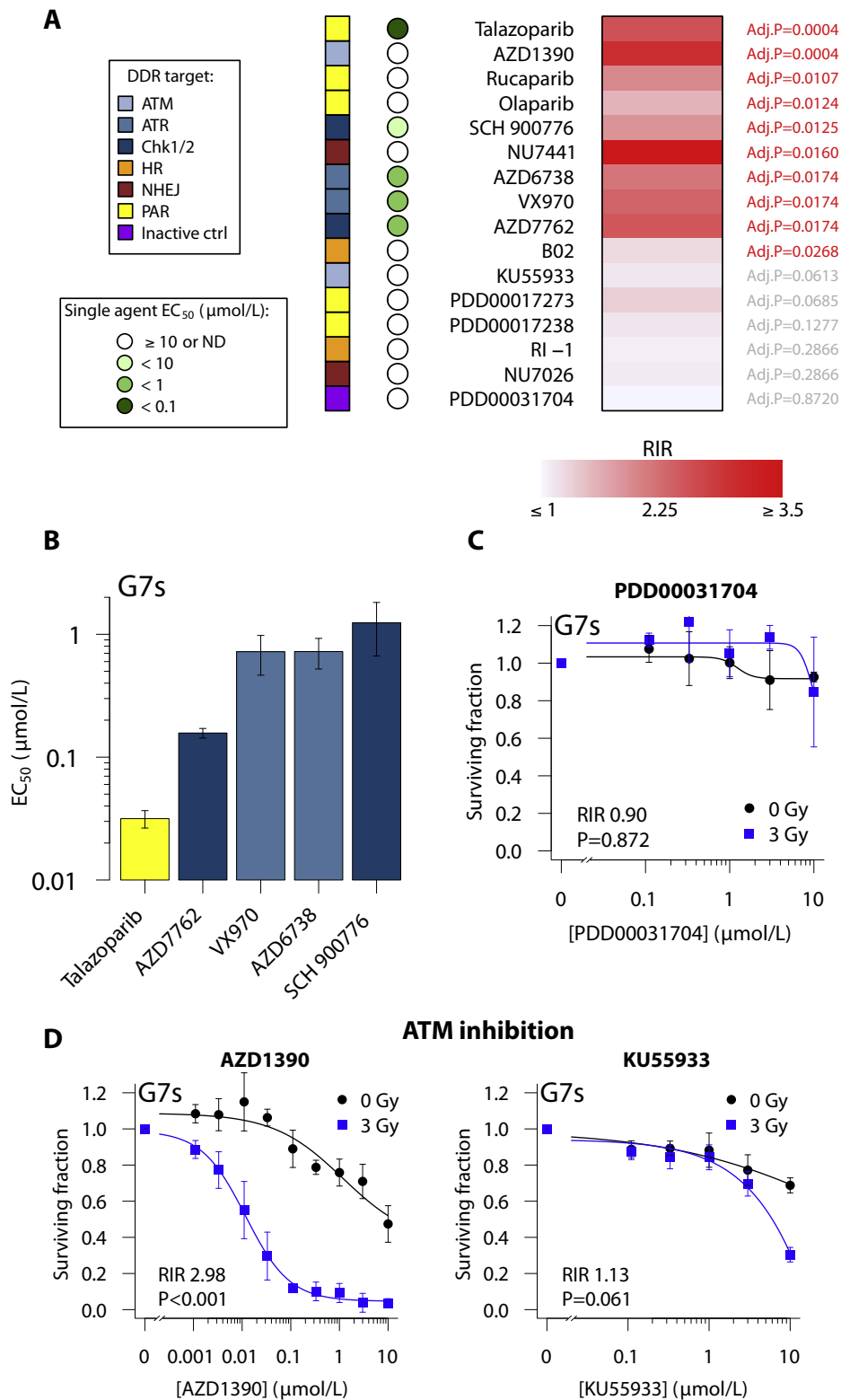


Fig. 4. Quantitative comparison of the radiation interaction of DNA damage response inhibitors using the ClonoScreen3D platform. (A) A panel of DNA damage response inhibitors was screened for interaction with radiation using the ClonoScreen3D platform in G7s cells. Cells were incubated with drugs for 2 hours before irradiation (3 Gy). Radiation interaction ratio values were computed and compounds ranked by false discovery rate (FDR)-adjusted *P* value, after 1-tailed ratio *t* testing. Drug single agent activity was quantified as half maximal effective concentration (EC₅₀) after fitting of a 4-parameter dose response model to sham-irradiated samples. The target pathway or protein is indicated. Data generated in 3 independent experiments. (B) DNA damage response inhibitors demonstrating single agent activity in G7s cells. Bars represent EC₅₀ with

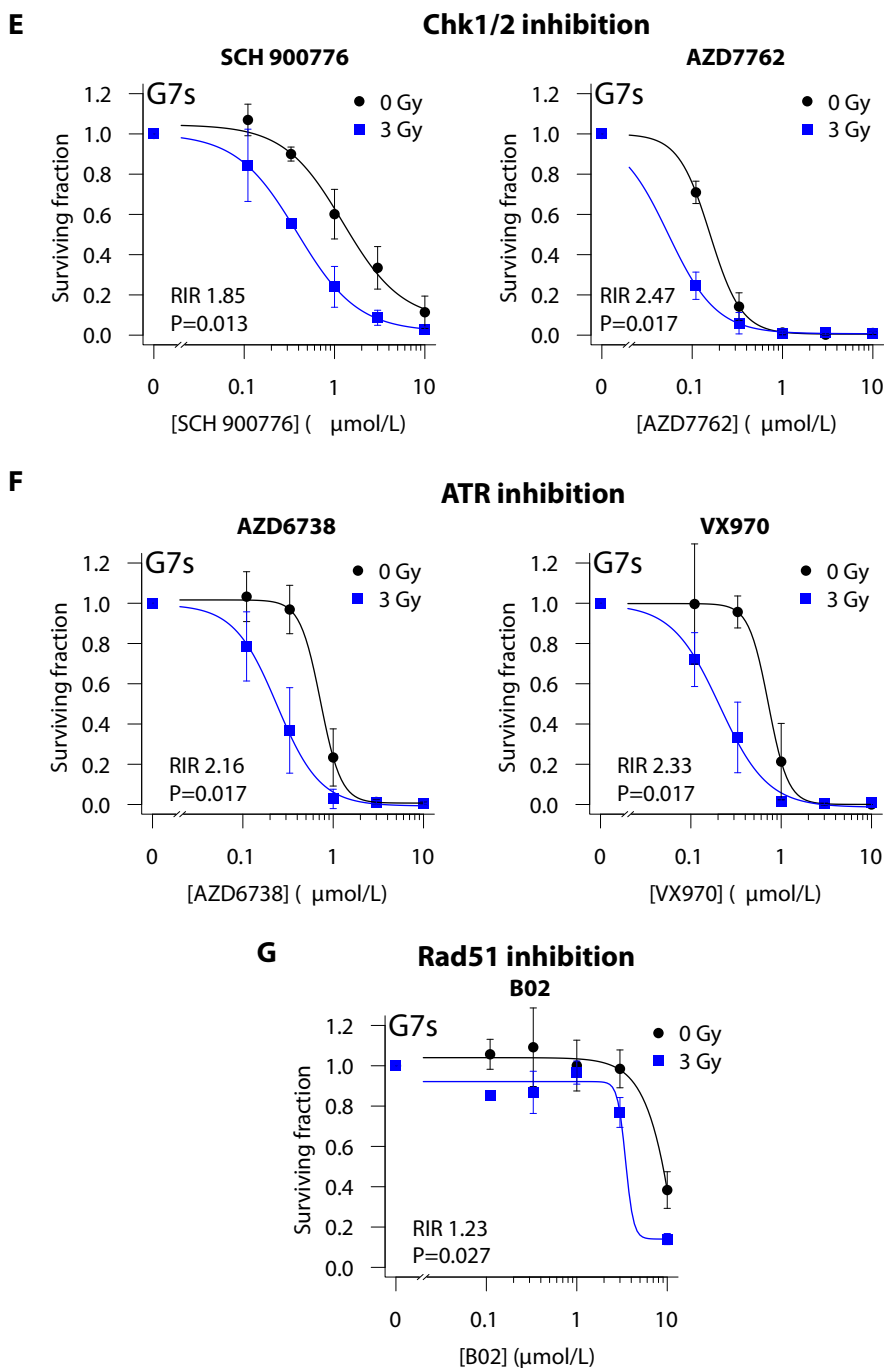


Fig. 4. Continued.

error bars indicating 95% CI. (C) Clonogenic survival of G7s cells treated with an inactive control compound, PDD00031704, and IR (3 Gy). (D) Clonogenic survival of G7s cells treated with Ataxia-telangiectasia mutated (ATM) inhibitors and IR (3 Gy). (E) Clonogenic survival of G7s cells treated with Chk1/2 inhibitors and IR (3 Gy). (F) Clonogenic survival of G7s cells treated with Ataxia Telangiectasia and Rad3-related protein (ATR) inhibitors and IR (3 Gy). (G) Clonogenic survival of G7s cells treated with the homologous recombination inhibitor B02 and IR (3 Gy). The surviving fraction of irradiated samples was computed using the plating efficiency of the vehicle + 3 Gy control, normalizing for the effect of radiation alone. Data fitted with a 4-parameter dose response curve. Points represent mean \pm SD, n = 3. *Abbreviations:* HR = homologous recombination; IR = ionizing radiation; ND = not determined; NHEJ = nonhomologous end-joining; PAR = poly(ADP-ribose); RIR = radiation interaction ratio.

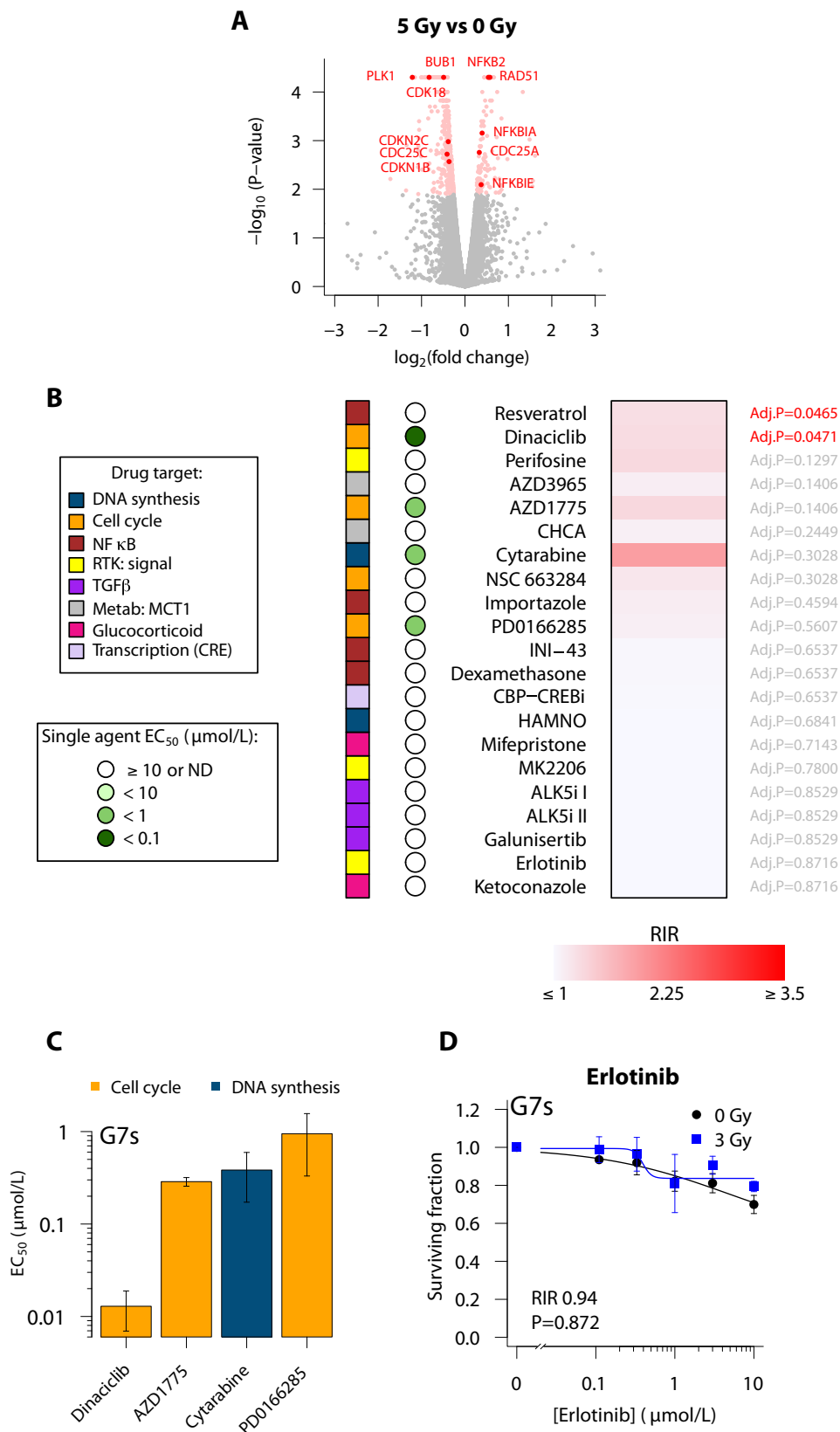


Fig. 5. Evaluation of drug-radiation combinations using the ClonoScreen3D platform for identification of novel radiosensitizers. (A) Transcriptomic changes in G7m cells cultured in 3-dimensional conditions were measured 4 hours after exposure to 5 Gy. Selected significantly upregulated and downregulated genes of interest are annotated, $n = 3$. (B) A panel of commercially available inhibitors targeting pathways identified by transcriptomic analysis was screened for interaction with radiation using the ClonoScreen3D platform in G7s cells. Cells were incubated with drugs for 2 hours before irradiation (3 Gy). Radiation

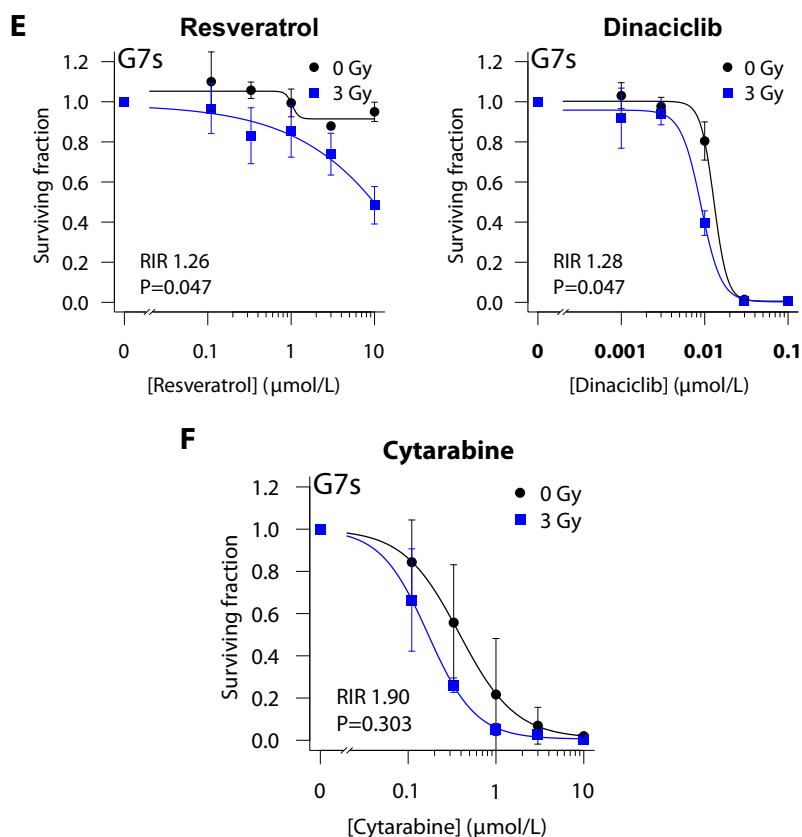


Fig. 5. Continued.

selected for evaluation as potential radiosensitizers using ClonoScreen3D (Table E3). Where several genes from the same biologic pathway were identified, additional compounds targeting the pathway were included, such as the WEE1 inhibitor AZD1775 to target mitosis and the cyclin-dependent kinase (CDK) inhibitor dinaciclib for cell cycle progression.

In this prospective screen, inhibitors targeting cell cycle regulation, in particular the G2/M checkpoint, demonstrated marked SAA in G7s cells (Figs. 5B,C and E5, Table E7). Dinaciclib, a potent small molecule inhibitor of CDK1, CDK2, CKD5, and CDK9, exhibited the highest SAA (EC_{50} 13 nmol/L; 95% CI, 4-21 nmol/L). Inhibitors targeting mitotic progression (AZD1775, PD0166285) also

showed potent SAA, as did cytarabine, a pyrimidine nucleoside analog that inhibits DNA synthesis.^{9,36} A similar pattern of SAA was observed in G7m cells (Fig. E6, Table E8).

Targeting DNA synthesis and CDKs induces radiosensitization of GBM cells

In keeping with previous 3D CSA and clinical trials,^{9,36} erlotinib exhibited no SAA or radiation interaction in G7s (RIR 0.94; $P = .872$; Fig. 5D) or G7m cells (RIR 1.06; $P = .104$; Fig. E6). Of the compounds targeting radiation-response processes identified by transcriptomic analysis, only 2 exhibited a robust interaction with

interaction ratio values were computed and compounds ranked by false discovery rate (FDR)-adjusted P value, after 1-tailed ratio t testing. Drug single agent activity was quantified as half maximal effective dose (EC_{50}) after fitting of a 4-parameter dose response model to sham-irradiated samples. The target pathway or protein is indicated. Data generated in 3 independent experiments. (C) Inhibitors demonstrating single agent activity in G7s cells. Bars represent EC_{50} with error bars indicating 95% CI. (D) Clonogenic survival of G7s cells treated with erlotinib and IR (3 Gy). (E) Clonogenic survival of G7s cells treated with dinaciclib or resveratrol and IR (3 Gy). (F) Clonogenic survival of G7s cells treated with cytarabine and IR (3 Gy). The surviving fraction of irradiated samples was computed using the plating efficiency of the vehicle + 3 Gy control, normalizing for the effect of radiation alone. Data fitted with a 4-parameter dose response curve. Points represent mean \pm SD, $n = 3$. *Abbreviations:* CRE = cAMP response element; DDR = DNA damage response; IR = ionizing radiation; Metab = metabolism; RIR = radiation interaction ratio; RTK = receptor tyrosine kinase.

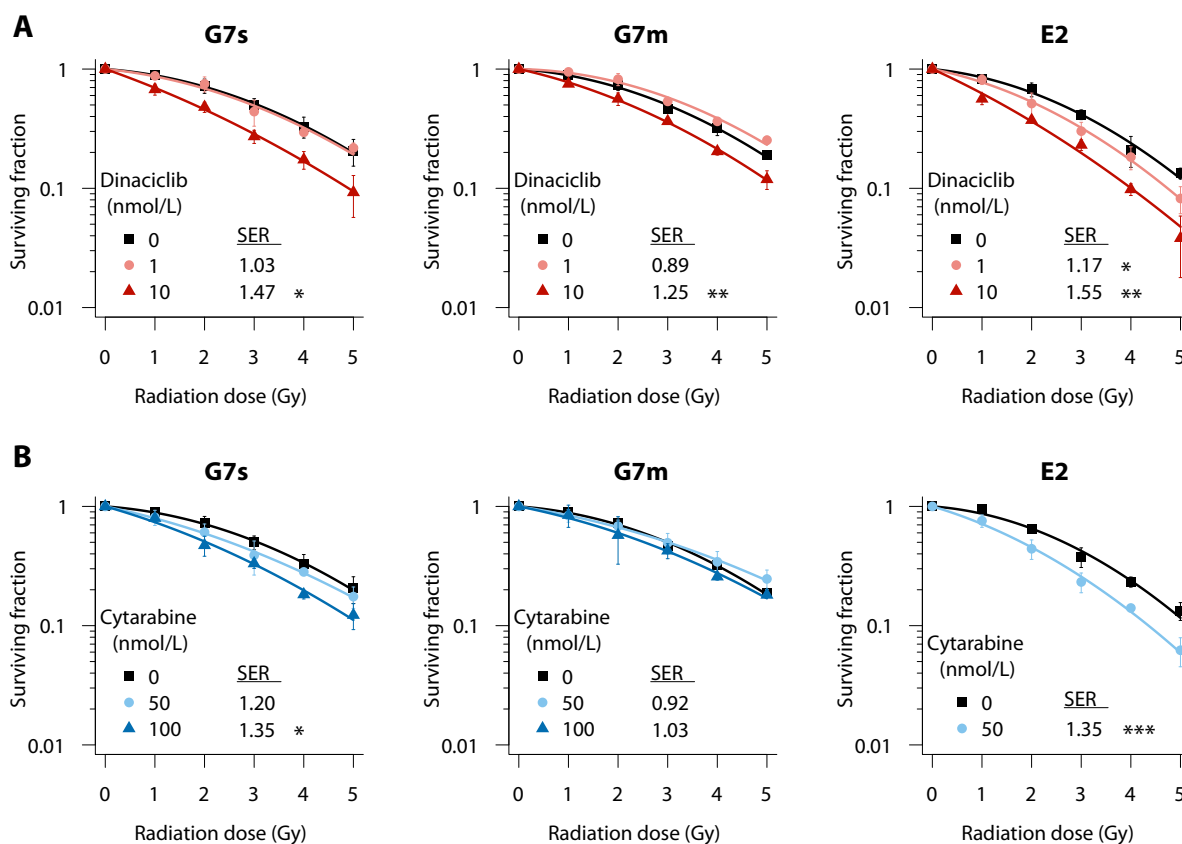


Fig. 6. Dinaciclib and cytarabine exhibit radiosensitizing activity in GBM cells. (A) Full 3-dimensional radiation dose response clonogenic survival of G7s, G7m, and E2 GBM cells treated with dinaciclib (1 and 10 nmol/L) 2 hours before ionizing radiation. (B) Full 3-dimensional radiation dose response clonogenic survival of G7s, G7m, and E2 GBM cells treated with cytarabine (50 and 100 nmol/L) 2 hours before ionizing radiation. Data fitted using the linear quadratic model. Sensitizer enhancement ratios calculated using linear quadratic mean inactivation dose and subject to 1-tailed ratio *t* test. Points represent mean \pm SD, *n* = 3. *Abbreviation:* GBM = glioblastoma; SER = sensitizer enhancement ratios.

radiation after correction of *P* values for multiple comparison. Resveratrol, an NF κ B inhibitor, demonstrated a modest interaction with IR in G7s cells (RIR 1.26; *P* = .047; Fig. 5E). In addition to potent SAA, dinaciclib exhibited an interaction with IR in G7s cells (RIR 1.28; *P* = .047). Despite failing to achieve statistical significance because of inter-replicate variability, the DNA synthesis inhibitor cytarabine exhibited the highest RIR value in this screen, in both G7s and G7m cells (G7s: RIR 1.90; *P* = .303; G7m: RIR 1.76; *P* = .104; Figs. 5F and E6). Because the RIR magnitude was high, the interaction with IR was additionally tested by statistical comparison of EC₅₀ values between the combination and radiation-only samples. A significant reduction in EC₅₀ was observed when cytarabine was combined with IR in G7m (*P* = .017) but not G7s (*P* = .119) cells (Fig. E7). This result and the SAA of cytarabine justified its selection for further investigation.

To confirm the ability of the ClonoScreen3D platform to identify bona fide novel radiosensitizers, gold-standard full radiation dose response CSAs (12-well) were performed for the novel hit compounds dinaciclib and cytarabine. Dinaciclib significantly radiosensitized G7s (SER 1.47; *P* = .010),

G7m (SER 1.25; *P* = .002), and E2 (SER 1.55; *P* = .001) cells at 10 nmol/L, with E2 cells also radiosensitized at 1 nmol/L (SER 1.17; *P* = .031; Fig. 6A and Table E9).

Significant radiosensitization was also elicited by cytarabine (100 nmol/L) in G7s (SER 1.35; *P* = .020) but not G7m cells (Fig. 6B). E2 cells were significantly radiosensitized by cytarabine at 50 nmol/L (SER 1.35; *P* = .001). These studies confirmed concentration-dependent radiosensitizing activity of dinaciclib and cytarabine in primary GBM cells cultured in 3D.

Discussion

Preclinical research is urgently required to identify therapeutic strategies for GBM that will translate into the clinic. Radiation therapy is a mainstay of GBM treatment but does not achieve cure, and radiation dose escalation is prohibited by lack of efficacy and normal brain toxicity.³⁷ The development of combination strategies to selectively sensitize GBM cells to IR is an attractive approach but has been severely

limited by the low throughput and/or low fidelity of the pre-clinical models currently available.

We have successfully refined an *in vitro* 3D model of GBM with demonstrable clinical relevance for use as a screening platform for novel radiation therapy drug combinations, with gold standard clonogenic survival as the readout. This is a major advance on existing screens involving IR, which generally rely on cell proliferation or short-term viability as readouts,³⁸ on combining cell proliferation with computational large-scale isobolographic analysis,³⁹ or on imaging readouts of longitudinal spheroid growth.^{40,41} These assays have limitations: (1) viability readouts fail to discriminate cells that have lost their capacity to reproduce indefinitely; (2) they are performed at early timepoints, measuring responses after only 1 or 2 mitoses, whereas radiation-induced damaged cells may divide several times before succumbing to reproductive death; (3) or, in the context of spheroid models, alterations in structure due to treatment may lead to the formation of enlarged spheroids, posing a challenge in accurately interpreting the response. The CSA is the only bona fide long-term reproductive integrity assay and hence the most clinically relevant.

Increasing the throughput of radiosensitizer identification experiments required reformatting of the CSA, a feat made possible by the increased growth surface area of 3D scaffold systems allowing statistically robust colony counts, in contrast to a 2D assay. Importantly, conversion of the ClonoScreen3D platform to 96-well format did not significantly influence treatment responses – a limitation reported previously.^{18,42} This enabled the platform to compare a broad range of DDR inhibitors as well as enabling screening of expansive drug libraries in 3D cultures of primary GBM cells for this first time.

A novel analytical parameter, the RIR, was developed based on established radiobiological approaches to enable flexible, reproducible, and statistically quantifiable assessment of the interactions between radiation and drugs, even when drug activity is not known a priori. Although modestly overestimating magnitude (reducing the likelihood of false-negative results), the RIR values for PARPi correlated with SER values determined using full CSA, confirming the utility of this novel parameter. In contrast to EC₅₀ comparison, well-defined SAA drug activity is not required for RIR computation, rendering it highly advantageous for screening applications. This parameter accurately predicted activity of known radiosensitizers⁴³ and discriminated nonactive compounds (eg, PDD00031704,⁴⁴ erlotinib^{9,36}) included as negative controls. Pragmatically, the relative probabilities of false-negative and false-positive findings can be tuned through *P* value adjustment methodology. For example, the significance of dinaciclib's interaction with radiation was not maintained after *P* value correction in G7m cells, but it was subsequently validated as a true radiosensitizer. To ensure robustness, hits identified in the ClonoScreen3D assay should be subject to full radiation dose CSA, to confirm and quantify radiosensitizing activity.

A recently published 2D CSA screening methodology included an established GBM cell line.¹⁸ Comparison of this system with ClonoScreen3D suggested several advantages of our platform, in addition to the notable improvement in clinical relevance offered by 3D culture.^{9,45} The method of Gomes et al¹⁸ required viral transduction for colony detection, which may have consequences for cell behavior. The assay also used high radiation doses (9 Gy) and a single drug concentration, meaning that narrow therapeutic combination windows may be missed. Furthermore, a secondary round of screening was required to distinguish between single agent and combination activity, whereas ClonoScreen3D quantifies both simultaneously and informs on drug concentrations for validation experiments. Lastly, the use of RIR to quantify drug-radiation interactions may be more intuitive and familiar to radiation biologists or oncologists than Z-score based metrics.

Given their critical role in the radiation response, inhibition of DDR proteins is expected to potentiate treatment efficacy.⁴⁶ As quantified by RIR, 13/15 (87%) of the DDR inhibitors tested showed a significant interaction with IR in at least 1 GBM cell context, confirming the assay's ability to detect potential radiosensitizing activity. The ClonoScreen3D platform also confirmed therapeutic interactions mediated by drugs targeting other pathways previously suggested to radiosensitize GBM cells, albeit in 2D conditions, for example, NFκB signalling (resveratrol).⁴⁷

ClonoScreen3D also identified novel radiosensitizing compounds including the Food and Drug Administration–approved compound dinaciclib. Dinaciclib is a selective and potent inhibitor of CDK1, CDK2, CDK5, and CDK9 with EC₅₀ values of 1 to 4 nmol/L across the target CDKs.⁴⁸ This compound has been well tolerated in clinical trials, exhibiting efficacy in patients with chronic lymphocytic leukemia⁴⁹ and relapsed multiple myeloma.⁵⁰ Consistent with our findings, SAA of dinaciclib has been previously reported in 2D and 3D GBM cells.^{51,52} A second Food and Drug Administration–approved drug, cytarabine, was also identified as a radiosensitizer. Cytarabine has exhibited clinical activity in 2 patients with astrocytoma after intraventricular administration of a liposomal formulation.⁵³ Regrettably, this study was terminated prematurely because of slow recruitment. Crucially, after identification by ClonoScreen3D, dinaciclib and cytarabine were validated as true radiosensitizers in the gold-standard radiation dose-response 3D CSA.

Undertaking medium or high throughput clonogenic survival screens in 2D culture is largely unworkable because of insufficient surface area in each well of a 96-well plate. The large increase in surface area (and hence colony numbers) per well provided by 3D culture systems provides an immediate advantage for radiosensitization studies. Three-dimensional systems have also shown biologic superiority over 2D cultures in terms of reproducing therapy response-relevant phenotypes, such as membrane microtubule formation, and predicting clinical efficacy.^{9,10,36} Consistent with this, the epidermal growth factor receptor inhibitor erlotinib, which showed

radiosensitizing activity in 2D culture but no efficacy in clinical trials,^{7,9} was successfully rejected by the ClonoScreen3D assay. The use of ClonoScreen3D is thus anticipated to reduce development of ineffective drugs that display spurious radiosensitizing activity in 2D culture.

The work presented here describes a novel drug-screening methodology for identification of radiosensitizers using cell culture technology that reproduces clinical treatment responses. This technology allowed comparison of multiple compounds undergoing evaluation in clinical trials. Our findings support the notion that targeting the DDR is likely to provide multiple opportunities for radiosensitization of GBM, for example with inhibitors of PARP (talazoparib), ATM (AZD1390), DNA-PK (NU7441), and Chk1 (SCH900776 and AZD7762), as long as they exhibit sufficient tumor penetration and do not exacerbate neurotoxicity.

Inhibitors of other DDR proteins, for example PARG, interacted with IR in a cell context-dependent manner, confirming the need to validate compounds in multiple primary cell lines. Finally, the paucity of translatable inhibitors of HR repair⁵⁴ was highlighted by the screen. The majority of non-DDR targeting drugs included in our initial screen showed little radiosensitizing potential, highlighting the strategic importance of DDR modulators. Advantageously, ClonoScreen3D allows newly identified candidate drugs to be benchmarked against established radiosensitizers.

Conclusion

The current dismal prognosis despite aggressive treatment suggests that novel combination approaches will have a crucial role in GBM therapy. Our results validate the ClonoScreen3D assay platform for identification and comparison of novel radiosensitizers for GBM, which has clear potential for extension to other cancer types. This assay provides a new technology that will underpin an improved drug development pipeline, accelerating development of lead compounds to augment the efficacy of radiation therapy.

References

- Louis DN, Perry A, Reifenberger G, et al. The 2016 World Health Organization classification of tumors of the central nervous system: A summary. *Acta Neuropathol* 2016;131:803-820.
- Stupp R, Hegi ME, Mason WP, et al. Effects of radiotherapy with concomitant and adjuvant temozolomide versus radiotherapy alone on survival in glioblastoma in a randomised phase III study: 5-year analysis of the EORTC-NCIC trial. *Lancet Oncol* 2009;10:459-466.
- Taylor OG, Brzozowski JS, Skelding KA. Glioblastoma multiforme: An overview of emerging therapeutic targets. *Front Oncol* 2019;9:963.
- Lassman AB, Abrey LE, Gilbert MR. Response of glioblastomas to EGFR kinase inhibitors. *New Engl J Med* 2006;354:525-526.
- Lai A, Tran A, Nghiemphu PL, et al. Phase II study of bevacizumab plus temozolomide during and after radiation therapy for patients with newly diagnosed glioblastoma multiforme. *J Clin Oncol* 2011;29:142-148.
- Rearidon DA, Neyns B, Weller M, et al. Cilengitide: An RGD pentapeptide alphanubeta3 and alphanubeta5 integrin inhibitor in development for glioblastoma and other malignancies. *Future Oncol* 2011;7:339-354.
- Vogelbaum MA, Peereboom D, Stevens G, Barnett G, Brewer C. Response rate to single agent therapy with the EGFR tyrosine kinase inhibitor erlotinib in recurrent glioblastoma multiforme: Results of a phase II study. *Neuro-Oncol* 2004;6:384.
- Mason WP. End of the road: Confounding results of the CORE trial terminate the arduous journey of cilengitide for glioblastoma. *Neuro Oncol* 2015;17:634-635.
- Gomez-Roman N, Stevenson K, Gilmour L, Hamilton G, Chalmers AJ. A novel 3D human glioblastoma cell culture system for modeling drug and radiation responses. *Neuro Oncol* 2017;19:229-241.
- Caragher S, Chalmers AJ, Gomez-Roman N. Glioblastoma's next top model: Novel culture systems for brain cancer radiotherapy research. *Cancers (Basel)* 2019;11:44.
- Walker MD, Green SB, Byar DP, et al. Randomized comparisons of radiotherapy and nitrosoureas for the treatment of malignant glioma after surgery. *New Engl J Med* 1980;303:1323-1329.
- Biau J, Chautard E, Verrelle P, Dutreix M. Altering DNA repair to improve radiation therapy: Specific and multiple pathway targeting. *Front Oncol* 2019;9:1009.
- Zhao B, Rothenberg E, Ramsden DA, Lieber MR. The molecular basis and disease relevance of non-homologous DNA end joining. *Nat Rev Mol Cell Biol* 2020;21:765-781.
- Scully R, Panday A, Elango R, Willis NA. DNA double-strand break repair-pathway choice in somatic mammalian cells. *Nat Rev Mol Cell Biol* 2019;20:698-714.
- Bao S, Wu Q, McLendon RE, et al. Glioma stem cells promote radioresistance by preferential activation of the DNA damage response. *Nature* 2006;444:756-760.
- Ahmed SU, Carruthers R, Gilmour L, Yildirim S, Watts C, Chalmers AJ. Selective inhibition of parallel DNA damage response pathways optimizes radiosensitization of glioblastoma stem-like cells. *Cancer Res* 2015;75:4416-4428.
- Ye R, Qiao Y, Singh PK, et al. High-content clonogenic survival screen to identify chemoradiation sensitizers. *Int J Radiat Oncol Biol Phys* 2021;111:e27-e37.
- Gomes NP, Frederick B, Jacobsen JR, Chapnick D, Su TT. A high throughput screen with a clonogenic endpoint to identify radiation modulators of cancer. *Radiat Res* 2023;199:132-147.
- Tiwana GS, Prevo R, Buffa FM, et al. Identification of vitamin B₁ metabolism as a tumor-specific radiosensitizing pathway using a high-throughput colony formation screen. *Oncotarget* 2015;6:5978-5989.
- Katz D, Ito E, Lau KS, et al. Increased efficiency for performing colony formation assays in 96-well plates: Novel applications to combination therapies and high-throughput screening. *Biotechniques* 2008;44:ix-xiv.
- Lin SH, Zhang J, Giri U, et al. A high content clonogenic survival drug screen identifies MEK inhibitors as potent radiation sensitizers for KRAS mutant non-small-cell lung cancer. *J Thorac Oncol* 2014;9:965-973.
- Al-Mayhany TMF, Ball SLR, Zhao J-W, et al. An efficient method for derivation and propagation of glioblastoma cell lines that conserves the molecular profile of their original tumours. *J Neurosci Methods* 2009;176:192-199.
- Ekström CT. MESS: Miscellaneous esoteric statistical scripts (ekstroem.github.io). 2019.
- Schaarschmidt GD. mratios: Ratios of coefficients in the general linear model (bris.ac.uk). 2018.
- Ritz C, Baty F, Streibig JC, Gerhard D. Dose-response analysis using R. *PLoS One* 2015;10:e0146021.
- Geissmann Q. OpenCFU, a new free and open-source software to count cell colonies and other circular objects. *PLoS One* 2013;8:e54072.
- Fang XG, Huang Z, Zhai K, et al. Inhibiting DNA-PK induces glioma stem cell differentiation and sensitizes glioblastoma to radiation in mice. *Sci Transl Med* 2021;13:eabc7275.

28. Jackson MR, Ashton M, Koessinger AL, Dick C, Verheij M, Chalmers AJ. Mesothelioma cells depend on the antiapoptotic protein Bcl-xL for survival and are sensitized to ionizing radiation by BH3-mimetics. *Int J Radiat Oncol Biol Phys* 2020;106:867-877.
29. Subiel A, Ashmore R, Schettino G. Standards and methodologies for characterizing radiobiological impact of high-Z nanoparticles. *Theranostics* 2016;6:1651-1671.
30. Hanna C, Kurian KM, Williams K, et al. Pharmacokinetics, safety and tolerability of olaparib and temozolomide for recurrent glioblastoma: Results of the phase I OPARATIC trial. *Neuro Oncol* 2020;22:1840-1850.
31. Chalmers AJ. Overcoming resistance of glioblastoma to conventional cytotoxic therapies by the addition of PARP inhibitors. *Anticancer Agents Med Chem* 2010;10:520-533.
32. Jannetti SA, Carlucci G, Carney B, et al. PARP-1-targeted radiotherapy in mouse models of glioblastoma. *J Nucl Med* 2018;59:1225-1233.
33. Venere M, Hamerlik P, Wu Q, et al. Therapeutic targeting of constitutive PARP activation compromises stem cell phenotype and survival of glioblastoma-initiating cells. *Cell Death Differ* 2014;21:258-269.
34. Sim HW, Galanis E, Khasraw M. PARP inhibitors in glioma: A review of therapeutic opportunities. *Cancers (Basel)* 2022;14:1003.
35. Lesueur P, Chevalier F, El-Habr EA, et al. Radiosensitization Effect of talazoparib, a parp inhibitor, on glioblastoma stem cells exposed to low and high linear energy transfer radiation. *Sci Rep* 2018;8:3664.
36. Gomez-Roman N, Chong MY, Chahal SK, et al. Radiation responses of 2D and 3D glioblastoma cells: A novel, 3D-specific radioprotective role of VEGF/Akt signaling through functional activation of NHEJ. *Mol Cancer Ther* 2020;19:575-589.
37. Greene-Schloesser D, Robbins ME, Peiffer AM, Shaw EG, Wheeler KT, Chan MD. Radiation-induced brain injury: A review. *Front Oncol* 2012;2:73.
38. Willers H, Pan X, Borgeaud N, et al. Screening and validation of molecular targeted radiosensitizers. *Int J Radiat Oncol Biol Phys* 2021;111:e63-e74.
39. Verrelle P, Gestraud P, Poyer F, et al. Integrated high-throughput screening and large-scale isobolographic analysis to accelerate the discovery of radiosensitizers with greater selectivity for cancer cells. *Int J Radiat Oncol Biol Phys* 2023. <https://doi.org/10.1016/j.ijrobp.2023.09.044>. Published online September 29.
40. Anastasov N, Hofig I, Radulovic V, et al. A 3D-microtissue-based phenotypic screening of radiation resistant tumor cells with synchronized chemotherapeutic treatment. *BMC Cancer* 2015;15:466.
41. Korovina I, Vehlou A, Temme A, Cordes N. Targeting integrin alpha2 as potential strategy for radiochemosensitization of glioblastoma. *Neuro Oncol* 2023;25:648-661.
42. Esquer H, Zhou Q, Abraham AD, LaBarbera DV. Advanced high-content-screening applications of clonogenicity in cancer. *SLAS Discov* 2020;25:734-743.
43. Gorte J, Beyreuther E, Danen EHJ, Cordes N. Comparative proton and photon irradiation combined with pharmacological inhibitors in 3D pancreatic cancer cultures. *Cancers (Basel)* 2020;12:3216.
44. James DI, Smith KM, Jordan AM, et al. First-in-class chemical probes against poly(ADP-ribose) glycohydrolase (PARG) inhibit DNA repair with differential pharmacology to olaparib. *ACS Chem Biol* 2016;11:3179-3190.
45. Storch K, Eke I, Borgmann K, et al. Three-dimensional cell growth confers radioresistance by chromatin density modification. *Cancer Res* 2010;70:3925-3934.
46. Rominiyi O, Collis SJ. DDRugging glioblastoma: Understanding and targeting the DNA damage response to improve future therapies. *Mol Oncol* 2022;16:11-41.
47. Wang L, Long L, Wang W, Liang Z. Resveratrol, a potential radiation sensitizer for glioma stem cells both in vitro and in vivo. *J Pharmacol Sci* 2015;129:216-225.
48. Parry D, Guzi T, Shanahan F, et al. Dinaciclib (SCH 727965), a novel and potent cyclin-dependent kinase inhibitor. *Mol Cancer Ther* 2010;9:2344-2353.
49. Flynn J, Jones J, Johnson AJ, et al. Dinaciclib is a novel cyclin-dependent kinase inhibitor with significant clinical activity in relapsed and refractory chronic lymphocytic leukemia. *Leukemia* 2015;29:1524-1529.
50. Kumar SK, LaPlant B, Chng WJ, et al. Dinaciclib, a novel CDK inhibitor, demonstrates encouraging single-agent activity in patients with relapsed multiple myeloma. *Blood* 2015;125:443-448.
51. Jane EP, Premkumar DR, Cavaleri JM, Sutera PA, Rajasekar T, Pollack IF. Dinaciclib, a cyclin-dependent kinase inhibitor promotes proteasomal degradation of Mcl-1 and enhances ABT-737-mediated cell death in malignant human glioma cell lines. *J Pharmacol Exp Ther* 2016;356:354-365.
52. Riess C, Koczan D, Schneider B, et al. Cyclin-dependent kinase inhibitors exert distinct effects on patient-derived 2D and 3D glioblastoma cell culture models. *Cell Death Discov* 2021;7:54.
53. Frankel BM, Cachia D, Patel SJ, Das A. Targeting subventricular zone progenitor cells with intraventricular liposomal encapsulated cytarabine in patients with secondary glioblastoma: A report of two cases. *SN Compr Clin Med* 2020;2:836-843.
54. Durant ST, Zheng L, Wang Y, et al. The brain-penetrant clinical ATM inhibitor AZD1390 radiosensitizes and improves survival of preclinical brain tumor models. *Sci Adv* 2018;4:eaat1719.